

Local spectral properties of Luttinger liquids: scaling versus nonuniversal energy scales

D Schuricht¹, S Andergassen^{1,2} and V Meden¹

¹Institut für Theorie der Statistischen Physik, RWTH Aachen University and
JARA—Fundamentals of Future Information Technology, 52056 Aachen, Germany

²Faculty of Physics, University of Vienna, Boltzmannngasse 5, 1090 Wien, Austria

E-mail: meden@physik.rwth-aachen.de

Abstract. Motivated by recent scanning tunneling and photoemission spectroscopy measurements on self-organized gold chains on a germanium surface we reinvestigate the local single-particle spectral properties of Luttinger liquids. In the first part we use the bosonization approach to exactly compute the local spectral function of a simplified field theoretical low-energy model and take a closer look at scaling properties as a function of the ratio of energy and temperature. Translational invariant Luttinger liquids as well as those with an open boundary (cut chain geometry) are considered. We explicitly show that the scaling functions of both setups have the same analytic form. The scaling behavior suggests a variety of consistency checks which can be performed on measured data to experimentally verify Luttinger liquid behavior. In a second part we approximately compute the local spectral function of a microscopic lattice model—the extended Hubbard model—close to an open boundary using the functional renormalization group. We show that as a function of energy and temperature it follows the field theoretical prediction in the low-energy regime and point out the importance of nonuniversal energy scales inherent to any microscopic model. The spatial dependence of this spectral function is characterized by oscillatory behavior and an envelope function which follows a power law both in accordance with the field theoretical continuum model. Interestingly, for the lattice model we find a phase shift which is proportional to the two-particle interaction and not accounted for in the standard bosonization approach to Luttinger liquids with an open boundary. We briefly comment on the effects of several one-dimensional branches cutting the Fermi energy and Rashba spin-orbit interaction.

PACS numbers: 71.10.Fd, 71.10.Pm, 78.47.-p, 79.60.i

1. Introduction

Over decades theoretical studies of the single-particle spectral properties of metallic one-dimensional (1d) correlated electron systems—so-called Luttinger liquids (LLs)—were ahead of the experimental attempts to find or synthesize appropriate quasi 1d materials and perform spectroscopy on them. In fact, while at the beginning of the 1990's a clear picture of the basic spectroscopic properties of translational invariant LLs was established (for reviews see e.g. Refs. [1], [2] and [3]) this period witnessed the first serious attempts to experimentally verify the specific spectroscopic signatures of LLs [4]. These are the (i) low-energy power-law suppression of the local spectral function $\rho(\omega) \sim |\omega|^\alpha$ for energies ω close to the chemical potential [5, 6, 7] with α depending on the two-particle interaction as well as (ii) the appearance of two dispersing features in the momentum resolved spectral function $\rho(k, \omega)$ (spin-charge separation) [8, 9, 10] instead of a single quasi-particle peak of a Fermi liquid. For finite temperatures T the suppression of the spectral weight as a function of ω is cut off by T and one finds the scaling behavior $\rho \sim T^\alpha S_\alpha(\omega/T)$ with a α -dependent scaling function S_α in which the two energy scales ω and T only enter via their ratio [11]. These results were exclusively obtained using bosonization within the Tomonaga-Luttinger (TL) model [1, 2, 3].

Using the modern language of renormalization group (RG) methods the (translational invariant) TL model is the exactly solvable effective low-energy fixed point model for a large class of metallic 1d correlated electron systems—the LLs [12]. It thus plays the same role as the free Fermi gas in Fermi liquid theory. The model has two strictly linear branches of right- and left-moving fermions and two-particle scattering is restricted to processes with small momentum transfer $|q| \ll k_F$, with the Fermi momentum k_F . These processes as well as the kinetic energy can be written as quadratic forms of the densities of right- and left-moving fermions which obey bosonic commutation relations. In most calculations in addition the momentum dependence of the low-momentum scattering processes g_2 and g_4 are neglected and momentum integrals are regularized in the ultraviolet introducing a cutoff 'by hand' (for an exception see Ref. [9]). One can extend the resulting *scale-free*, field theoretical model by allowing for additional two-particle scattering processes. These turn out to be RG irrelevant in a wide parameter regime [13]. The most important of these processes is the so-called $g_{1,\perp}$ -process (in the g-ology classification [13]) with momentum transfer $2k_F$ between two scattering fermions of opposite spin.

In some of the early experiments on 1d chains these were obviously interrupted by local impurities [4]. A simple model of an *inhomogeneous* LL is the open boundary analog of the TL model. Interestingly, a LL is very susceptible towards single-particle perturbations with momentum transfer $2k_F$ [7] and on asymptotically low energy scales even a single weak impurity has the same effects on the spectral properties as an open boundary [14]. Triggered by this theoretical insight and the early experiments, the spectral properties of the open boundary analog of the TL model were studied [15, 16]. The local spectral function close to the boundary shows power-law behavior as a function

of ω but with an exponent α_B different from the bulk one α . As in the translational invariant case in this model only those low-energy scattering terms are kept which can be written as quadratic forms in bosonic densities. Only recently it was shown that a large class of further two-particle processes appearing in a 1d system with an open boundary are indeed RG irrelevant [17].

The latest scanning tunneling spectroscopy (STS) and photoemission spectroscopy (PES) measurements on different classes of 1d metallic systems [18, 19, 20, 21, 22] impressively demonstrated that the experiments caught up and more refined questions must now be answered by theory. Important ones are: How do effects which are not captured by the low-energy fixed point model, such as the momentum dependence of the two-particle interaction and the nonlinearity of the single-particle dispersion influence the spectral functions? What is the energy scale of a given microscopic model on which the low-energy LL physics sets in? How do scaling functions for lattice models look like in detail? Here we shed some light on the last two questions and briefly comment on the first one. It is widely believed that neglecting the momentum dependence of the interaction and regularizing momentum integrals in the ultraviolet 'by hand' has no effect on the low-energy physics of LL's. This is indeed correct if all energy scales are sent to zero, that is for $\rho(\omega)$ and $\rho(\pm k_F, \omega)$: at small ω the spectral properties are unaffected by the details of the momentum dependence of the g 's. However, if $\rho(k, \omega)$ as a function of ω is studied at fixed $k \neq \pm k_F$, as it is usually done in angular resolved PES, details of the momentum dependence of the interaction matter. This was investigated in Ref. [23]. An overview on the effects of the nonlinearity of the single-particle dispersion can be found in the very recent review Ref. [24].

This paper is organized as follows. In Sect. 2 we compute the local spectral function of the translationally invariant *and* the open boundary continuum TL model using bosonization. We show that both display scaling in ω/T and that the scaling functions have the same analytic form. We next compute the spectral function of the extended Hubbard model on the lattice close to an open boundary as a function of energy, temperature and position in Sect. 3. For this an approximate method is used which is based on the functional RG approach [25]. It is devised for weak to intermediate two-particle interactions. In particular, we concentrate on inhomogeneous LLs as the boundary exponent α_B characterizing the spectral function close to an open boundary is *linear* in the two-particle interaction while the bulk exponent is *quadratic* (see below). Varying the microscopic parameters of the extended Hubbard model we can tune the strength of the different scattering processes and thus study the crossover between nonuniversal behavior and the low-energy LL physics. We perform a scaling analysis of the spectral function as a function of ω and T and show that the spectral weight close to the boundary follows the bosonization prediction within the universal low-energy regime. The position dependence of the spectral function is characterized by oscillatory behavior and a power-law envelope function in accordance with the result for the TL. Interestingly, we additionally find a phase shift which is proportional to the two-particle interaction and not accounted for in the standard bosonization procedure.

We summarize our results in Sect. 4 and briefly comment on how spin-orbit interaction and several bands crossing the Fermi surface—both being potentially important effects in recent experiments—influence the single-particle spectral functions.

2. Scaling functions of the Tomonaga-Luttinger model

In this section we derive closed analytic expressions for the single-particle Green function and the related local spectral function of the TL model with and without an open boundary at finite T . We then closely inspect the scaling form of the spectral functions.

In field theoretical notation (see e.g. Ref. [26]) the Hamiltonian density of the TL model in spin-charge separated form reads

$$\mathcal{H}(x) = \sum_{\nu=c,s} \mathcal{H}_\nu(x), \quad \mathcal{H}_\nu = \frac{v_\nu}{16\pi} \left[\frac{1}{K_\nu} (\partial_x \Phi_\nu)^2 + K_\nu (\partial_x \Theta_\nu)^2 \right], \quad (1)$$

with the canonical Bose fields Φ_ν and their dual fields Θ_ν . Within the TL model the charge and spin velocities $v_{c,s}$ as well as the LL parameters $K_{c,s}$ are free parameters. If the model is used to describe the low-energy physics of an underlying microscopic model they become functions of the corresponding model parameters and the band filling [1, 2, 3]. For spin-rotational invariant models on which we focus in the present and the next section $K_s = 1$. For repulsive interactions $0 < K_c < 1$ while $K_c > 1$ in the attractive case. Here we exclusively consider the former. The field operator $\Psi_\sigma(x)$ annihilating an electron with spin direction $\sigma = \uparrow, \downarrow$ at position x is decomposed into a right- and a left-moving part

$$\Psi_\sigma(x) = e^{ik_F x} R_\sigma(x) + e^{-ik_F x} L_\sigma(x). \quad (2)$$

The imaginary time fields R_σ and L_σ are bosonized according to

$$R_\sigma^\dagger(\tau, x) = \frac{\eta_\sigma}{\sqrt{2\pi}} \exp\left(\frac{i}{2}\phi_c(\tau, x)\right) \exp\left(\frac{i}{2}f_\sigma\phi_s(\tau, x)\right), \quad (3)$$

$$L_\sigma^\dagger(\tau, x) = \frac{\eta_\sigma}{\sqrt{2\pi}} \exp\left(-\frac{i}{2}\bar{\phi}_c(\tau, x)\right) \exp\left(-\frac{i}{2}f_\sigma\bar{\phi}_s(\tau, x)\right), \quad (4)$$

where the Klein factors η_σ satisfy anticommutation rules $\{\eta_\sigma, \eta_{\sigma'}\} = 2\delta_{\sigma,\sigma'}$ and $f_\uparrow = 1 = -f_\downarrow$. The fields ϕ_ν and $\bar{\phi}_\nu$ are the chiral components of Φ_ν and Θ_ν ,

$$\Phi_\nu = \phi_\nu + \bar{\phi}_\nu, \quad \Theta_\nu = \phi_\nu - \bar{\phi}_\nu, \quad \nu = c, s. \quad (5)$$

For the translational invariant TL model the Hamiltonian follows by integrating the density Eq. (1) over \mathbb{R} . The TL model with an open boundary is obtained by integrating the density Eq. (1) over $x \geq 0$ and employing the boundary condition $\Psi_\sigma(x=0) = 0$ for the fermionic and $\Phi_{c,s}(x=0) = 0$ for the bosonic fields, respectively.

We are here interested in the imaginary time-ordered single-particle Green function

$$G_{\sigma\sigma'}(\tau, x_1, x_2) = - \left\langle \mathcal{T}_\tau \Psi_\sigma(\tau, x_1) \Psi_{\sigma'}^\dagger(0, x_2) \right\rangle, \quad (6)$$

where $\langle \dots \rangle$ denotes the expectation value in the canonical ensemble. From the decomposition Eq. (2) it follows that

$$G_{\sigma\sigma'} = e^{ik_F(x_1-x_2)} G_{\sigma\sigma'}^{RR} + e^{-ik_F(x_1-x_2)} G_{\sigma\sigma'}^{LL} + e^{ik_F(x_1+x_2)} G_{\sigma\sigma'}^{RL} + e^{-ik_F(x_1+x_2)} G_{\sigma\sigma'}^{LR}, \quad (7)$$

where, for example $G_{\sigma\sigma'}^{RL} = -\langle \mathcal{T}_\tau R_\sigma(\tau, x_1) L_{\sigma'}^\dagger(0, x_2) \rangle$. As we are aiming at the local spectral function, we eventually set $x_1 = x_2 = x$. For the translational invariant TL model the left- and right-moving fermion fields are independent and thus $G_{\sigma\sigma'}^{RL} = G_{\sigma\sigma'}^{LR} = 0$. In the presence of an open boundary the above mentioned boundary conditions imply $R_\sigma(\tau, x) = -L_\sigma(\tau, -x)$. In this case and after setting $x_1 = x_2 = x$ the cross terms are characterized by a fast spatial oscillation with frequency $2k_F$.

Using standard methods (see e.g. Ref. [2]) one obtains for the Green function of a translational invariant system ($K_s = 1$, $\tau > 0$, $\beta = 1/T$, $r = x_1 - x_2$, $R = (x_1 + x_2)/2$)

$$G_{\sigma\sigma'}^{RR}(\tau, x_1, x_2) = -\frac{\delta_{\sigma,\sigma'}}{2\pi} \left(\frac{\pi}{v_c\beta}\right)^{a+b} \left(\frac{\pi}{v_s\beta}\right)^{1/2} \frac{1}{\sin^{1/2} \left[\frac{\pi}{v_s\beta} (v_s\tau - ir) \right]} \quad (8)$$

$$\times \frac{1}{\sin^a \left[\frac{\pi}{v_c\beta} (v_c\tau - ir) \right]} \frac{1}{\sin^b \left[\frac{\pi}{v_c\beta} (v_c\tau + ir) \right]}$$

$$G_{\sigma\sigma'}^{LL}(\tau, x_1, x_2) = G_{\sigma\sigma'}^{RR}(\tau, x_2, x_1) \quad (9)$$

and for the case with boundary

$$[G_{\sigma\sigma'}^{RR}]_B(\tau, x_1, x_2) = G_{\sigma\sigma'}^{RR}(\tau, x_1, x_2) \left\{ \frac{\sinh\left(\frac{2\pi}{v_c\beta}x_1\right) \sinh\left(\frac{2\pi}{v_c\beta}x_2\right)}{\sin\left[\frac{\pi}{v_c\beta}(v_c\tau - 2iR)\right] \sin\left[\frac{\pi}{v_c\beta}(v_c\tau + 2iR)\right]} \right\}^c \quad (10)$$

$$[G_{\sigma\sigma'}^{LL}]_B(\tau, x_1, x_2) = [G_{\sigma\sigma'}^{RR}]_B(\tau, x_2, x_1) \quad (11)$$

The cross terms $[G_{\sigma\sigma'}^{RL}]_B$ and $[G_{\sigma\sigma'}^{LR}]_B$ are equal to $-[G_{\sigma\sigma'}^{RR}]_B$ and $-[G_{\sigma\sigma'}^{LL}]_B$ after interchanging $r \leftrightarrow 2R$. The appearing exponents are given by

$$a = \frac{1}{8} \left(\sqrt{K_c} + \frac{1}{\sqrt{K_c}} \right)^2, \quad b = \frac{1}{8} \left(\sqrt{K_c} - \frac{1}{\sqrt{K_c}} \right)^2, \quad c = \frac{1}{8} \left(\frac{1}{K_c} - K_c \right). \quad (12)$$

The main steps to obtain the local spectral function from the imaginary time Green function are the analytic continuation $\tau \rightarrow it + \delta$ followed by Fourier transformation with respect to t . Mathematically the real part δ corresponds to the ultraviolet cutoff introduced to regularize momentum integrals. From an experimental perspective it can be considered as the resolution of the setup (at $T = 0$).

For the translational invariant model one obtains ($x_1 = x_2 = x$)

$$\begin{aligned} \rho(\omega, x) &= -\frac{1}{2\pi} (1 + e^{-\beta\omega}) \sum_{\sigma,\sigma'} \int_{-\infty}^{\infty} dt e^{i\omega t} [G_{\sigma\sigma'}^{RR}(\tau, x, x) + G_{\sigma\sigma'}^{LL}(\tau, x, x)] \Big|_{\tau \rightarrow it + \delta} \\ &= \frac{1}{\pi^2} (1 + e^{-\beta\omega}) \left(\frac{\pi}{v_c\beta}\right)^{a+b} \left(\frac{\pi}{v_s\beta}\right)^{1/2} \int_{-\infty}^{\infty} dt \frac{e^{i\omega t}}{\sin^{a+b+1/2} \left(\frac{\pi\tau}{\beta} \right)} \Big|_{\tau \rightarrow it + \delta} \\ &= \frac{4\pi^{a+b+1/2}}{\pi^2 v_c^{a+b} v_s^{1/2}} T^a S_a(\omega/T), \end{aligned} \quad (13)$$

with

$$S_\gamma(u) = 2^{1+\gamma} \Gamma(-\gamma) \sin[\pi(1+\gamma)] \cosh\left(\frac{u}{2}\right) \left| \Gamma\left(\frac{1+\gamma}{2} + i\frac{u}{2\pi}\right) \right|^2, \quad (14)$$

$$\alpha = a + b - \frac{1}{2} = \frac{1}{4} \left(K_c + \frac{1}{K_c} - 2 \right). \quad (15)$$

The *position independent* local spectral weight of the translational invariant TL model thus shows *scaling behavior*: $T^{-\alpha} \rho(\omega, x)$ is a function of ω/T only. The amplitude of the scaling function depends on $v_{c/s}$ and K_c , which in turn are functions of the interaction strength, while its shape is given by K_c only. This result was first derived in Ref. [11]. A similar expression was later used to describe transport properties of LLs [27].

Taking the $T \rightarrow 0$ limit of Eq. (13) one obtains the well known power-law suppression of the spectral weight [5, 6, 7]

$$T = 0: \quad \rho(\omega, x) \sim |\omega|^\alpha, \quad (16)$$

for $|\omega| \rightarrow 0$. For fixed small $T > 0$ this is cut off by temperature and ρ saturates for $|\omega| \lesssim T$. For the energy set to the chemical potential, that is $\omega = 0$, one finds a power-law suppression of ρ for $T \rightarrow 0$ (see Eq. (13)): $\rho \sim T^\alpha$. From studies of microscopic models it is known that (see e.g. Ref. [3])

$$K_c = 1 - \frac{U}{U_m} + \mathcal{O}\left(\left[\frac{U}{U_m}\right]^2\right), \quad (17)$$

where U is a measure of the two-particle interaction and U_m is a scale which depends on the other model parameters. Using Eq. (15) one thus obtains

$$\alpha \sim U^2, \quad (18)$$

for the exponent characterizing the low-energy behavior of the local spectral function of the translational invariant TL model.

Verifying the power-law suppression of the spectral weight as a function of T and ω with the same exponent α as well as the scaling property of measured STS and/or PES data provide strong indications that the system under investigation is indeed a LL [22]. It was very recently argued that these characteristics are still not unique to LLs as other mechanisms than 1d electronic correlations might lead to similar behavior [28]. We therefore suggest further consistency checks by in addition measuring spectra close to the end points of cut 1d chains.

The local spectral function becomes position x dependent when considering a chain with an open boundary. In this case $\rho(\omega, x)$ has three contributions

$$\rho_B(\omega, x) = \rho_0(\omega, x) + e^{2ik_F x} \rho_{2k_F}(\omega, x) + e^{-2ik_F x} \rho_{-2k_F}(\omega, x), \quad (19)$$

where the first follows from Fourier transforming $G^{RR} + G^{LL}$ and the last two from transforming G^{RL} and G^{LR} , respectively ($x_1 = x_2 = x$). Following the same steps as above we obtain

$$\rho_0(\omega, x) = \frac{\pi^{a+b+1/2}}{\pi^2 v_c^{a+b} v_s^{1/2}} T^{a+b-1/2} F(\omega/T, xT/v_c), \quad (20)$$

with

$$F(u, v) = \int_{-\infty}^{\infty} ds \frac{e^{ius} (1 + e^{-u})}{\sin^{a+b+1/2}(i\pi s + \delta)} \left(\frac{\sinh^2(2\pi v)}{\sin(i\pi s - 2\pi iv + \delta) \sin(i\pi s + 2\pi iv + \delta)} \right)^c \quad (21)$$

and

$$\rho_{2k_F}(\omega, x) = \rho_{-2k_F}^*(\omega, x) = -\frac{\pi^{a+b+1/2}}{2\pi^2 v_c^{a+b} v_s^{1/2}} T^{a+b-1/2} G(\omega/T, xT/v_c), \quad (22)$$

where

$$G(u, v) = \int_{-\infty}^{\infty} ds \frac{e^{ius} (1 + e^{-u})}{\sin^{1/2}(i\pi s - 2\pi iv v_c/v_s + \delta)} \frac{1}{\sin^a(i\pi s - 2\pi iv + \delta)} \frac{1}{\sin^b(i\pi s + 2\pi iv + \delta)} \times \left(\frac{\sinh(2\pi v)}{\sin(i\pi s + \delta)} \right)^{2c}. \quad (23)$$

In the limit $T \rightarrow 0$ these expressions simplify to the ones given in Refs. [16] and [29].

For distances from the boundary beyond the thermal length $\sim 1/T$, that is $xT/v_c = v \gg 1$ we expect $\rho_B(\omega, x)$ to become equal to $\rho(\omega, x)$ of Eq. (13) (exponentially fast). That this is indeed the case follows from

$$\frac{xT}{v_c} \gg 1: \quad F(\omega/T, xT/v_c) \approx 4S_\alpha(\omega/T), \quad G(\omega/T, xT/v_c) \approx 0, \quad (24)$$

Eqs. (19), (20), (22) and (14). We thus end up with

$$\frac{xT}{v_c} \gg 1: \quad \rho_B(\omega, x) \approx \rho(\omega, x). \quad (25)$$

We next consider the limit $xT/v_c = v \ll 1$, that is the local spectral function close to the open boundary. Then

$$F(u, v) \approx (2\pi)^{2c} v^{2c} (1 + e^{-u}) \int_{-\infty}^{\infty} ds \frac{e^{ius}}{\sin^{a+b+2c+1/2}(i\pi s + \delta)}. \quad (26)$$

Interestingly the remaining integral has the same form as the one appearing in the second line of Eq. (13) but with $a + b + 1/2$ replaced by $a + b + 2c + 1/2$. For fixed x close to the boundary $\rho_0(x, \omega)$ thus displays scaling with the *same* scaling function as the one found in the bulk but α replaced by

$$\alpha_B = a + b + 2c - 1/2 = \frac{1}{2} \left(\frac{1}{K_c} - 1 \right). \quad (27)$$

Explicitely one obtains

$$\frac{xT}{v_c} \ll 1: \quad \rho_0(x, \omega) \sim x^{2c} T^{\alpha_B} S_{\alpha_B}(\omega/T). \quad (28)$$

With Eq. (17) the boundary exponent α_B Eq. (27) has, in contrast to the bulk one α , a contribution *linear* in the interaction

$$\alpha_B \sim U \quad (29)$$

and one finds $\alpha_B > \alpha$. To show that for fixed x close to the boundary $T^{-\alpha_B} \rho_B$ indeed follows the same scaling function as in the bulk (with $\alpha \rightarrow \alpha_B$) we still have to analyze

ρ_{2k_F} for $xT/v_c = v \ll 1$. In the simplest approximation we neglect the v -dependence in the integral Eq. (23) and obtain

$$\frac{xT}{v_c} \ll 1 : \quad \rho_{2k_F}(\omega, x) = -\frac{1}{2}\rho_0(\omega, x). \quad (30)$$

Using Eq. (19) this completes our proof that for fixed

$$x \text{ in the bulk:} \quad T^{-\alpha}\rho(\omega, x) = T^{-\alpha}\rho_B(\omega, x) \sim S_\alpha(\omega/T), \quad (31)$$

$$x \text{ close to the boundary:} \quad T^{-\alpha_B}\rho_B(\omega, x) \sim S_{\alpha_B}(\omega/T), \quad (32)$$

with S_γ given in Eq. (14).

Showing the consistency of the scaling of spectra measured in the two spatial regimes is within reach of the latest STS experiments [22]. Combined with a consistency check of the two exponents α and α_B , which both depend on K_c only and which was already achieved in Ref. [22] (see also Sect. 4), this would provide a stringent experimental verification of LL physics.

One can *improve* the analysis of ρ_{2k_F} close to the boundary by keeping the phase factor $\exp(i\kappa uv)$ of the integral Eq. (23).[‡] A numerical evaluation of the integral shows that κ is a function of K_c and v_c/v_s with $\kappa(K_c = 1, v_c/v_s = 1) = 2$. Taking all terms together we find

$$\begin{aligned} \frac{xT}{v_c} \ll 1 : \quad T^{-\alpha_B}\rho_B(\omega, x) = A x^{2c} \cosh\left(\frac{\omega}{2T}\right) \left| \Gamma\left(\frac{1+\alpha_B}{2} + i\frac{\omega}{2\pi T}\right) \right|^2 \\ \times \left\{ 1 - \cos\left[\left(2k_F + \frac{\kappa\omega}{v_c}\right)x\right] \right\}, \end{aligned} \quad (33)$$

where the overall amplitude A depends on K_c , v_c and v_s but *not* on the variables ω , x , and T .

In the $T \rightarrow 0$ limit Eqs. (19) to (23) give close to the boundary

$$T = 0, \quad \frac{x|\omega|}{v_c} \ll 1 : \quad \rho_B(\omega, x) \sim x^{2c} |\omega|^{\alpha_B} \left\{ 1 - \cos\left[\left(2k_F + \frac{\kappa\omega}{v_c}\right)x\right] \right\}. \quad (34)$$

At fixed x , ρ_B thus vanishes $\sim |\omega|^{\alpha_B}$. As in the translational invariant case this power law is cut off by a finite temperature and ρ_B saturates for $|\omega| \lesssim T$. For fixed x close to the boundary and $\omega = 0$ Eq. (32) gives $\rho_B \sim T^{\alpha_B}$ for $T \rightarrow 0$. At $T = 0$ and deep in the bulk, that is for $x|\omega|/v_c \gg 1$, $\rho_{\pm 2k_F}$ can be written as a sum of terms which vanish algebraically in x [16, 29]. They show a power-law dependence on $|\omega|$ in general each with a different exponent. The contribution ρ_0 to ρ_B becomes position independent and goes as $\rho_0 \sim |\omega|^\alpha$ (instead of α_B close to the boundary). For sufficiently large $x|\omega|/v_c$ (such that algebraically decaying terms can be neglected) one thus finds ($\omega \rightarrow 0$)

$$T = 0, \quad \frac{x|\omega|}{v_c} \gg 1 : \quad \rho_B(\omega, x) \sim |\omega|^\alpha. \quad (35)$$

For $T = 0$ and in the *noninteracting* limit $\rho_{\pm 2k_F}^0$ does not decay and one obtains

$$T = 0 : \quad \rho_B^0(\omega, x) = \frac{2}{\pi v_F} \left\{ 1 - \cos\left[2\left(k_F + \frac{\omega}{v_F}\right)x\right] \right\}, \quad (36)$$

[‡] We have verified numerically that the additional dependences of the integral Eq. (23) on u , v , and the model parameters are irrelevant for the regimes studied here.

for all x and ω .

It is often argued, that the contribution ρ_{2k_F} to ρ_B can be neglected when comparing to experiments. The electrons in PES and STS do not come from a specific location x but rather from an extended spatial range. If this is large enough compared to the characteristic length $1/k_F$, ρ_{2k_F} averages out due to the fast spatial oscillations with frequency $2k_F$. It is not obvious that the criterion for neglecting ρ_{2k_F} is fulfilled in the latest STS experiments [22] (see Sect. 4).

Equation (33) (or Eq. (34) for $T = 0$) allows for another consistency check of LL behavior. It predicts a spatial power-law dependence of ρ_B close to the boundary with exponent $2c = (1/K_c - K_c)/4$ superimposed by oscillations. If it is possible to measure the envelope function of the spatial dependence of the spectral weight close to a boundary and extract the power-law exponent it would allow to relate the resulting K_c to the ones obtained from α and/or α_B .

We note in passing that performing a spatial Fourier transform of $\rho_B(\omega, x)$ reveals characteristic informations of the bulk state of a LL including its elementary excitations (see Ref. [26] and references therein).

In the next section we show that the spectral function of microscopic lattice models of interacting 1d electrons, in our case the extended Hubbard model, indeed shows scaling behavior as a function of ω/T . Up to a subtlety in the spatial dependence, namely an interaction dependent phase shift in the oscillatory factor, the lattice spectral function falls on top of the above computed scaling function of the TL model. This holds in the low-energy regime. We discuss the crossover between this universal behavior and the nonuniversal regime at higher energies. The crossover scale Δ depends on the parameters of the microscopic model.

3. Spectral properties of the extended Hubbard model

Partly aiming at the low-energy LL physics of microscopic lattice models of interacting electrons different groups computed the local spectral function [30, 31] as well as the momentum resolved one [32, 33] for such models using very accurate numerical methods (often denoted as 'numerically exact'). Quantum Monte-Carlo (QMC) [30, 33] and (dynamical) density-matrix renormalization group (DMRG) [32, 31] were used. The results obtained by these methods turned out to be very useful for understanding the spectral features of the studied models over the entire band width. Unfortunately, due to system size restrictions (DMRG and QMC), artificial broadenings of the spectra (DMRG), as well as the problem of analytic continuation of numerical data (QMC), it was not possible to reach the low-energy regime; in none of the calculations it was possible to convincingly demonstrate power-law behavior of the spectra. Rephrasing this in experimental terms one can say that the energy resolution of these methods is not high enough. § For (partly) technical reasons the focus of the numerical approaches

§ For a very recent attempt to observe power-law behavior of the spectral function in a spinless lattice model using DMRG, see Ref. [34].

lies on the Hubbard model with a local two-particle interaction. As the crossover scale Δ between LL behavior and nonuniversal physics in this model is very small (see below) reaching the LL regime is particularly challenging.

We here use a method which allows to obtain *approximate* results for the spectral function of the extended Hubbard model with a local U and nearest-neighbor V interaction. Our approximation is based on the functional RG approach to quantum many-body physics [25]. Functional RG allows to set up a hierarchy of approximation schemes with the two-particle interaction being the small parameter. The one we are using here is controlled to leading order and can thus only be used for small to intermediate U and V (compared to the band width). The method was mainly applied in the context of transport through inhomogeneous LLs and there it was shown to reproduce typical impurity strength independent [14] LL exponents to *leading order* in the interaction [35, 36]. Due to appropriate resummations of classes of diagrams the RG procedure thus goes way beyond standard perturbation theory. As the exponent of the bulk local spectral function is of *second order* in the interaction (see Eq. (18)) the LL physics of translationally invariant systems cannot be assessed in our approximation. In the following we therefore restrict ourselves to the model with open boundaries characterized by the exponent α_B which has a *linear* contribution (see Eq. (29)) and study ρ_B *close* to one of the boundaries. We here refrain from giving any further technical details on how the spectral function can be computed within our functional RG approach. Those can be found in Ref. [36].

The Hamiltonian of the extended Hubbard model with two open boundaries is given by

$$H = -t \sum_{j=1}^{N-1} \sum_{\sigma} (c_{j+1,\sigma}^{\dagger} c_{j,\sigma} + c_{j,\sigma}^{\dagger} c_{j+1,\sigma}) + U \sum_{j=1}^N n_{j,\uparrow} n_{j,\downarrow} + V \sum_{j=1}^{N-1} n_j n_{j+1}, \quad (37)$$

where $c_{j,\sigma}^{\dagger}$ and $c_{j,\sigma}$ are creation and annihilation operators for fermions with spin σ on lattice site j , while $n_{j,\sigma} = c_{j,\sigma}^{\dagger} c_{j,\sigma}$, and $n_j = n_{j,\uparrow} + n_{j,\downarrow}$ is the local density operator on site j . For the (nonextended) Hubbard model the nearest neighbor interaction V vanishes. The number of lattice sites is denoted by N . The noninteracting tight-binding part gives the standard dispersion $\epsilon_k = -2t \cos k$ with the hopping matrix element $t > 0$ (the lattice constant is chosen to be unity).

Under the *assumption* that a given microscopic model is a LL (at low energy scales) one can use general relations between the exact ground state energy E_0 and K_c [12, 1, 2, 3] to extract the dependence of the LL parameter K_c on the parameters of the model considered. In general however E_0 of a many-body system is not known analytically. The translational invariant Hubbard model constitutes one of the rare exceptions and closed expressions for E_0 in form of integral equations can be determined using Bethe ansatz [37]. The integral equations can easily be solved numerically which gives access to the dependence of K_c on the parameters U/t and the band filling n (n can vary between 0 and 2) [38]. We emphasize that this *only* implies that on *asymptotically*

small scales one can expect power-law behavior with α (bulk) or α_B (close to the boundary) while no information on the crossover scale Δ from nonuniversal to universal LL behavior can be extracted this way. Furthermore, this expectation holds under the assumption that the Hubbard model is a LL, which away from half-filling $n = 1$ —for which it is a Mott insulator [37]—is not doubted seriously, but also not proven rigorously. For the (translational invariant) extended Hubbard model $K_c(U/t, V/t, n)$ can only be computed numerically along similar lines [39]. The exponents α and α_B for the Hubbard [38] cannot become large enough to match the exponents inferred from experiments on different systems [18, 19, 20, 21, 22], or, putting it differently, K_c cannot become small enough. For the extended Hubbard model K_c 's of roughly the correct order can be achieved for U and V of the order of the band width or larger. This part of the parameter space lies very close to the Mott transition of the model [39]. One can expect that this effects the spectral properties. When aiming at a typical LL spectral function with α and α_B of experimental size it is thus advisable to study models with interaction of longer spatial range. We note that within our approximate approach U and V are bound to be sufficiently smaller than the band width. The extended Hubbard model is spin-rotational invariant which implies $K_s = 1$.

For the Hubbard model with an open boundary the scale Δ was earlier computed in the small U limit and it was estimated to be exponentially small [40]

$$\frac{\Delta}{v_F k_F} = \exp \left\{ -\frac{\pi v_F}{U} \ln \frac{1 + [U/(8v_F)]^2}{[U/(8v_F)]^2} \right\}. \quad (38)$$

In fact, approaching the chemical potential $\omega \rightarrow 0$ the local spectral weight first increases before the LL power-law suppression sets in for $|\omega| \lesssim \Delta$ (see the solid line in Fig. 1 which does not look 'LL-like' around $\omega = 0$; the power-law suppression is beyond the energy resolution). This is consistent with the observation of a small crossover scale and a peak close to $\omega = 0$ in the local spectra of the *translational invariant* Hubbard model obtained numerically by QMC and DMRG [30, 31].

To compute the finite temperature $\rho_B(\omega, j)$ (here the continuous position x is replaced by the discrete lattice site index j) of the extended Hubbard model we consider a chain of N lattice sites described by Eq. (37). For this the spectrum is discrete and the spectral function consists of δ -peaks. Due to even-odd effects the spectral weight might vary quickly from one eigenvalue to the next one. A smooth function of ω is obtained by averaging the weight over neighboring eigenvalues. To obtain the local spectral function as defined in the continuum one furthermore has to divide the weights by the level spacing between eigenvalues. The energy scale $\delta_N = \pi v_F/N$ associated to the chain length becomes irrelevant as we always consider sufficiently large systems with $T \gtrsim \delta_N$ for fixed T . Our results are thus not influenced by finite size effects (for an exception, see the discussion of Fig. 4). Typical experimental temperatures are in the few to few ten Kelvin range which corresponds to $T \approx 10^{-4}t$ to $10^{-3}t$ for our model.

|| A similar energy averaging is inherent to any STS or PES experiment due to the finite energy resolution of these techniques.

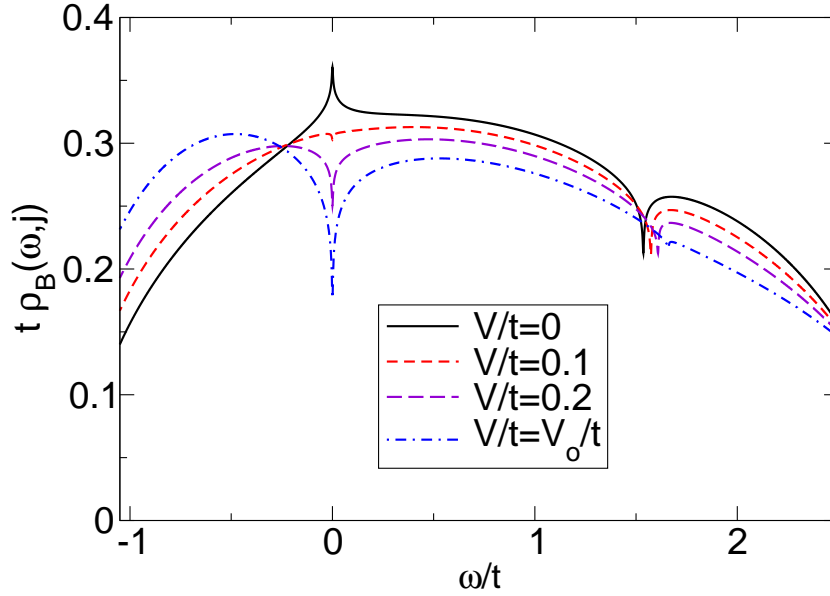


Figure 1. (Color online) Local spectral function of the extended Hubbard model for $n = 3/4$, $j = 1$, $U/t = 0.5$, $N = 2^{14}$, $T/t = 10^{-3}$ and different V/t . For filling $n = 3/4$ the optimal nearest-neighbor interaction is given by $V_o/t = U/(t\sqrt{2}) \approx 0.35$. Only for sizable nearest-neighbour interaction V we observe the LL suppression of the weight at $\omega = 0$. The suppression close to $\omega/t = 1.5$ is a lattice effect [41].

In Fig. 1 $\rho_B(\omega, j)$ is shown for filling $n = 3/4$, lattice site $j = 1$ next to the boundary, $U/t = 0.5$, $N = 2^{14}$, $T/t = 10^{-3}$ and different V/t . For the Hubbard model with $V/t = 0$ no suppression of the spectral weight is observable as Δ is much smaller than temperature. Obviously, Δ increases with increasing V/t and the LL suppression at $\omega = 0$ becomes apparent. This can be understood as follows. The crossover scale Δ is strongly affected by the size of the open boundary analog of a $g_{1,\perp}$ two-particle scattering process [17, 36, 40] which cannot be written quadratically in the bosonic densities. Its initial value (with respect to an RG flow) in the extended Hubbard model is given by $g_{1,\perp} = U + 2V \cos(2k_F)$ with $k_F = n\pi/2$. It is large for $V = 0$. At $V_o = -U/[2 \cos(2k_F)]$ it vanishes (see the dashed-dotted line in Fig. 1). Under an RG procedure this 'non-LL term' flows to zero and is thus RG irrelevant. However, the flow is only logarithmically. This implies that for sizable initial $g_{1,\perp}$ LL physics sets in on exponentially small scales consistent with Eq. (38) for the Hubbard model [40]. For small initial $g_{1,\perp}$, ρ_B appears LL-like with the characteristic power-law behavior of the spectral weight close to $\omega = 0$. In Fig. 1 the spectral weight at $\omega = 0$ remains finite due to the finite temperature. We conclude that to observe LL physics on moderate scales in the present model the interaction should not be too local. In particular, to demonstrate power-law behavior and obtain an estimate of the exponent by fitting ρ_B for fixed j (close to the boundary) and $T \ll t$ as a function of ω (in the range $T \ll |\omega| \ll t$) one should consider fine-tuned parameters with $V = V_o$. The spectral functions of Fig. 1 show another 'high-energy' nonanalyticity. A similar feature was observed for a model

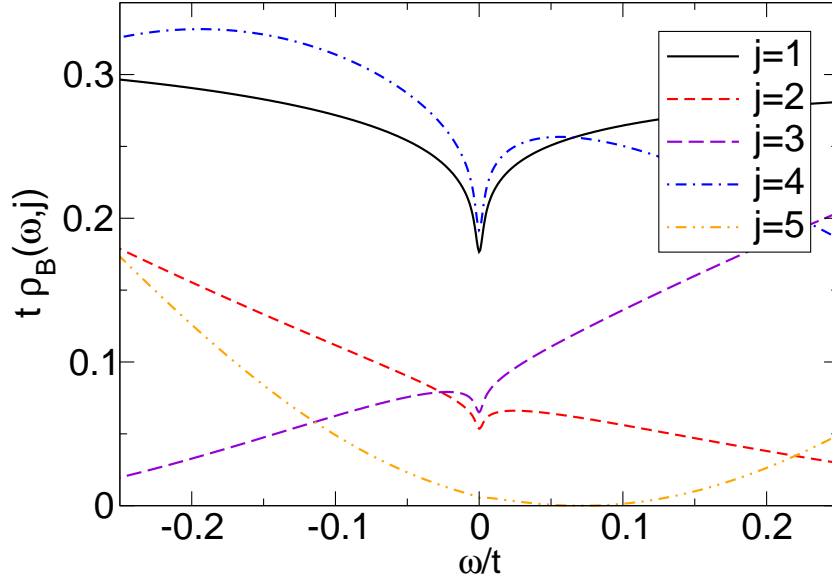


Figure 2. (Color online) Low-energy regime of the local spectral function of the extended Hubbard model for $n = 3/4$, $U/t = 0.5$, $V = V_o = U/\sqrt{2}$ (for $n = 3/4$), $N = 2^{14}$, $T/t = 10^{-3}$ and different j close to the open boundary at $j = 1$.

of spinless fermions in Ref. [41] and was explained there as a lattice effect.

In Fig. 2 the low-energy regime of ρ_B is shown for the same parameters as in Fig. 1 but 'optimal' $V = V_o = U/\sqrt{2}$ (for $n = 3/4$), which allows for the largest low-energy regime, and varying position j close to the boundary site $j = 1$. For fixed ω we observe strong variations of the weight with j and pronounced $\omega \leftrightarrow -\omega$ asymmetries which is consistent with the result from the TL model Eq. (33). Below we return to the spatial dependence of ρ_B .

To confirm scaling in ω/T at fixed j as predicted in Eq. (33) we computed ρ_B for the parameters of Fig. 2 but with $j = 1$ and for different T . By fitting $\rho_B(\omega, j = 1)$ as a function of ω for the smallest T in the range $T \ll |\omega| \ll t$ we can extract a functional RG estimate of the boundary exponent α_B^{fRG} . For the given parameters we obtain $\alpha_B^{\text{fRG}} = 0.089$ in good agreement with the DMRG result $\alpha_B^{\text{DMRG}} = 0.095$ obtained from Eq. (27) and $K_c^{\text{DMRG}} = 0.840$ derived as explained above [39]. The scaling obtained with this α_B^{fRG} is shown in Fig. 3. In the inset the unscaled data are displayed. The thick solid line is the prediction Eq. (33) of the TL model with an open boundary, where we replaced $\alpha_B \rightarrow \alpha_B^{\text{fRG}}$. The data nicely collapse on the TL model curve in the low-energy regime.

We next take a closer look at the j dependence of ρ_B at fixed ω . As emphasized in the last section measuring the local spectral weight as a function of j offers another possibility for a consistency check that the system under consideration is a LL: Eq. (33) predicts power-law behavior of the envelope with exponent $2c = (1/K_c - K_c)/4$. Figure 4 shows ρ_B for $n = 3/4$, $U/t = 0.5$, $N = 2^{14}$, $T/t = 10^{-3}$ and $\omega \approx 0$ as a function of j (filled circles). Here $\omega \approx 0$ refers to taking the eigenvalue of the finite system

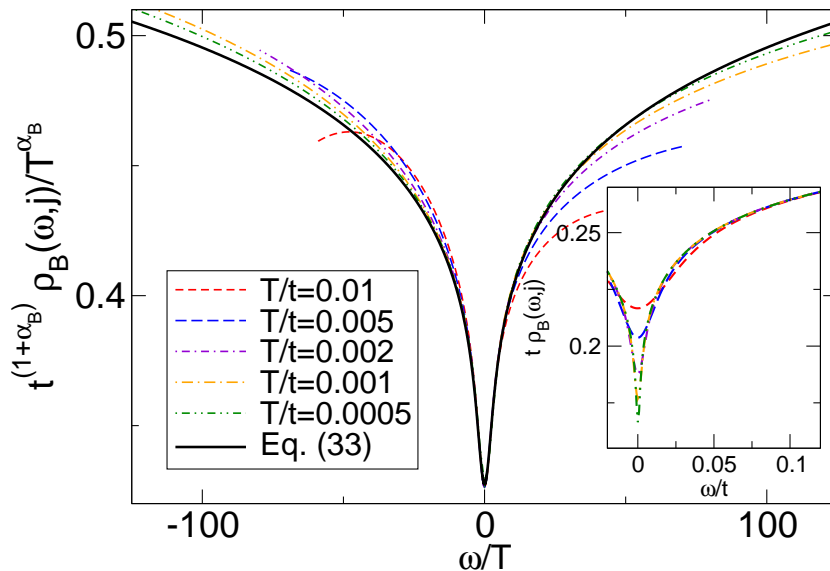


Figure 3. (Color online) Scaling plot of the local spectral function of the extended Hubbard model for $n = 3/4$, $U/t = 0.5$, $V = V_o = U/\sqrt{2}$ (for $n = 3/4$), $N = 2^{14}$, $j = 1$ and different T . The inset shows the unscaled spectral function as a function of ω for different T .

closest to $\omega = 0$, which might be of order $1/N$ away from zero. We again tune V to the optimal value $V_o = U/\sqrt{2}$ (for $n = 3/4$) providing the largest Δ . The spatial oscillations with frequency $2k_F = 3\pi/4$ are apparent. We fitted the envelope to a power law $\sim j^{2c^{\text{fRG}}}$ and obtained $2c^{\text{fRG}} = 0.087$ in excellent agreement with $2c^{\text{DMRG}} = (1/K_c^{\text{DMRG}} - K_c^{\text{DMRG}})/4 = 0.088$. The power-law fit is shown as the thick solid line in Fig. 4. As mentioned above we control the different exponents only to leading order in the interaction. To this order the analytic expressions for α_B and $2c$ agree, as is apparent from Eqs. (12), (27) and (17). The numerical values for $2c^{\text{fRG}}$ and α_B^{fRG} still differ by roughly 2% as the RG produces higher than linear order terms in the different exponents as well. We emphasize that for $V = 0$, that is for the Hubbard model, in a similar plot no spatial suppression of the envelope of the spectral weight at small j is visible. In fact, the envelope of the spectral weight at $\omega \approx 0$ even *increases* for j approaching the boundary site $j = 1$.

A comparison of the data for $U/t = 0.5$ (filled circles) and for $U/t = 0$ (crosses) additionally presented in Fig. 4 shows that a *phase shift* ξ of the spatial $2k_F$ oscillations appears which is *not* captured by the result for the TL model Eq. (33). The latter was derived using standard bosonization with the boundary conditions on the continuum fields given after Eq. (5). The deviation of the $U/t = 0$ curve from Eq. (36) for $j \gtrsim 20$ (splitting of degenerate values of the spectral weight) is a finite size effect; ω is not exactly zero but of order $1/N$ (eigenvalue closest to zero). The phase shift can be most easily identified from the observation that ρ_B vanishes on every eighth lattice site for $U/t = 0$ (crosses), as it is supposed to according to Eq. (36) with $\omega = 0$ and $2k_F = 3\pi/4$, but not so for $U/t = 0.5$ (filled circles), where the same should hold according to Eq. (33).

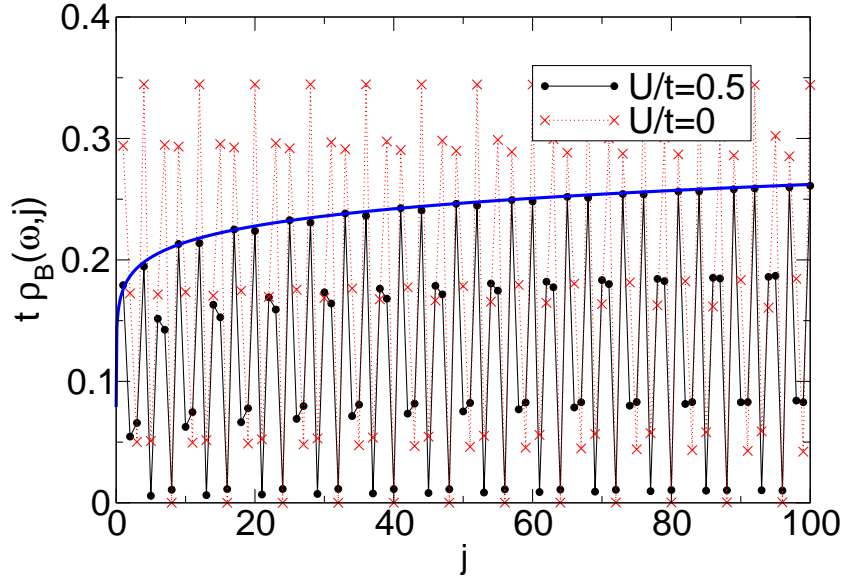


Figure 4. (Color online) Lattice site dependence of the spectral function of the extended Hubbard model close to the boundary site $j = 1$ for $n = 3/4$, two different U/t , $V = V_o = U/\sqrt{2}$ (for $n = 3/4$), $N = 2^{14}$, $T/t = 10^{-3}$ and $\omega \approx 0$. The solid line is a power-law fit to the envelope.

The phase ξ turns out to be *linearly* dependent on U (for small U/t and $V = V_o(U)$). As our functional RG approximation scheme is controlled to this order, the appearance of ξ is a reliable finding. Considering $T = 0$ at different system sizes N we furthermore verified that ξ does not vanish for decreasing $1/N$. The phase shift is thus not a finite size effect. A phase shift as observed in the extended Hubbard model (with $V = V_o(U)$) can be accounted for in bosonization by adding a *local single-particle forward scattering term* $W\delta(x)\partial_x\Phi_c(x)$ to the Hamiltonian density Eq. (1). The phase shift is then given by $2\pi K_c W/v_c$. To match the result of the extended Hubbard model (with $V = V_o(U)$) W has to be chosen U -dependent, in particular $W \sim U$ for small U/t . The STS and PES experiments always imply a spatial averaging. As the phase shift becomes illusive even after averaging over only a few lattice sites and as the main focus of the present paper is on relating theoretical spectral functions to experimental ones we here do not further investigate this issue.

Finally we compare the spatial dependence of ρ_B for two different ω in Fig. 5. Apparently the frequency of the spatial oscillations depends on ω which is consistent with Eq. (33). As this is more transparent for a 'more commensurable' filling, the parameters of this figure are $n = 2/3$, $U/t = 0.5$, $V = V_o = U$ (for $n = 2/3$), $N = 2^{14}$ and $T/t = 10^{-3}$.

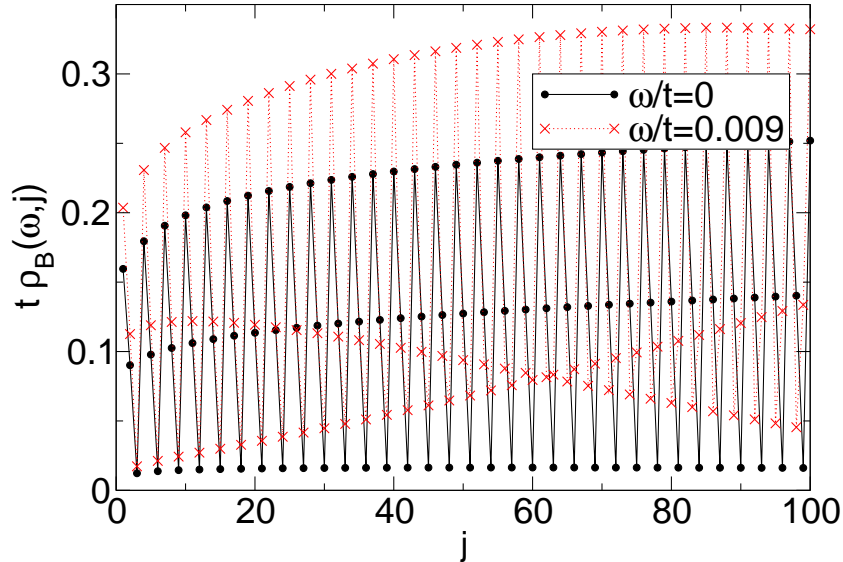


Figure 5. (Color online) Lattice site dependence of the spectral function of the extended Hubbard model close to the boundary site $j = 1$ for $n = 2/3$, two different ω , $U/t = 0.5$, $V = V_0 = U$ (for $n = 2/3$), $N = 2^{14}$, $T/t = 10^{-3}$.

4. Summary

In the first part of this paper we have derived analytic expressions for the power-law behavior of the local spectral weight ρ of the translational invariant TL model as well as the one with an open boundary ρ_B as a function of ω , T and x . The results provide a variety of possibilities for consistency checks of experimental STS and PES data on 1d electron systems. The first is to show scaling of data for different ω and T taken in the bulk or at fixed position close to the boundary onto the bosonization predictions Eqs. (13) and (15) (bulk) or Eq. (33) (boundary). Scaling of bulk spectra was e.g. demonstrated in Ref. [22]. If the same could be achieved for boundary spectra the *same* scaling function with α replaced by α_B should appear if the system is a LL. Experimentally showing this together with the required consistency of α and α_B (for a spin-rotational invariant model with $K_s = 1$ both given by a single number K_c ; see Eqs. (15) and (27)) would constitute a second highly nontrivial check that the studied system indeed is a LL. A consistency of bulk and boundary exponents within the experimental error bars (but not the entire scaling function) was achieved in Refs. [27] and [22] (also see below). A third consistency check is provided by the predicted spatial power-law behavior with the exponent $2c$ which again can be expressed solely in terms of K_c (see Eq. (12)).

It is often argued that the spatially oscillating contributions ρ_{2k_F} and ρ_{-2k_F} to ρ_B with frequency $2k_F$ can be neglected when comparing to experimental spectra due to spatial averaging effects. Taking the numbers from Ref. [22] this is not apparent. In this experiment $k_F \approx 5 \times 10^8/\text{m}$ while the range of spatial averaging is estimated as $\Delta x \approx 5 \times 10^{-9} \text{m}$, leading to $2k_F \Delta x = 5$. This is not a very large number and one

would thus conclude that ρ_{2k_F} and ρ_{-2k_F} cannot be dropped. A quantitative picture of the averaging effects can easily be obtained by integrating Eq. (19) over an appropriate spatial range. We have explicitly verified that averaging over $\Delta x \approx 5 \times 10^{-9}$ m does not significantly smear out the boundary ($x\omega/v_c \ll 1$) and bulk ($x\omega/v_c \gg 1$) exponents in ω at low temperatures (here $T = 0$). In particular, this shows that the spatial resolution of the experiment is high enough to detect α_B (as it is implicit to the analysis presented in Ref. [22]).

In connection with the comparison of the experimental results on gold chains on a germanium surface of Ref. [22] to the LL predictions one might be worried about two effects which are not included in the TL model of Sect. 2. One is Rashba spin-orbit interaction (SOI), which in a surface setup can become sizable. Along the lines of Refs. [42] and [43] one can bosonize the 1d electron gas with Rashba SOI. An important effect is the appearance of *two* different Fermi velocities $v_F(1 \pm \zeta)$ due to subband mixing and the SOI splitting [42, 43]. Here ζ is a measure of the strength of the SOI. The local spectral function (with and without an open boundary) shows the same characteristics as a function of ω as discussed in Sect. 2, but with modified exponents

$$\alpha^{\text{SOI}} = \alpha - \frac{(K_c - 1)^2}{2(1 + K_c)} \zeta + \mathcal{O}(\zeta^2), \quad (39)$$

$$\alpha_B^{\text{SOI}} = \alpha_B + \frac{K_c - 1}{K_c + 1} \zeta + \mathcal{O}(\zeta^2). \quad (40)$$

Taking realistic numbers for the velocities it turns out that $\zeta \ll 1$ and the effects of Rashba SOI on the exponents are negligible. We note in passing that also the momentum resolved spectral function of a translational invariant LL is barely modified by SOI of realistic size [44].

The other issue is the observation of *four* electron branches (instead of two in the TL model) crossing the Fermi surface in PES measurements on the gold chains [45]. The four branch situation can also be accounted for in bosonization [46, 47]. One then has to introduce even and odd pairs of charge and spin density bosons as well as the related K 's and velocities. Under the plausible *assumption* that only the even charge channel LL parameter is different from the noninteracting value 1, that is $K_{c,e} = K_c < 1$, one finds the same power-law behavior for the local spectral functions as a function of ω as the ones given in Sect. 2 but with

$$\alpha = \frac{1}{8} \left(K_c + \frac{1}{K_c} - 2 \right), \quad (41)$$

$$\alpha_B = \frac{1}{4} \left(\frac{1}{K_c} - 1 \right). \quad (42)$$

Interestingly taking these expressions would significantly improve the consistency of the experimentally determined α and α_B [22]. From the measured value $\alpha = 0.53$ of the bulk spectra one finds $\alpha_B = 1.27$ which nicely agrees to the measured value $\alpha_B = 1.20$. In particular, the agreement is improved compared to taking the two-branch expressions Eqs. (15) and (27) which gives $\alpha_B = 1.43$ [22].

In the second part of our paper we have shown that the behavior of ρ_B as a function of ω , T and j close to an open boundary predicted by the bosonization solution of the TL model can indeed be found in an example of a microscopic lattice model, namely the extended Hubbard model. Interestingly, a linear-in- U phase shift ξ not captured by standard open-boundary bosonization appears in the spatial oscillations of the spectral weight of the extended Hubbard model. The energy resolution required to access the low-energy LL regime strongly depends on the model parameters. Even for the fairly high energy resolution we can achieve within our approximate method, convincingly demonstrating LL power-law behavior and reliably extracting exponents requires fine-tuning of the parameters. Roughly speaking the crossover scale becomes small if the two-particle interaction becomes too local. This suggests that to access the low-energy LL regime at a given experimental energy resolution one should consider systems with poor screening properties.

Acknowledgements: We are grateful to Jörg Schäfer, Ralph Claessen, Kurt Schönhammer and Christian Ast for very fruitful discussions. The numerical calculations were performed on the machines of the Max-Planck Institute for Solid State Research, Stuttgart. This work was supported by the DFG via the Emmy-Noether program (D.S.) and FOR 723 (S.A. and V.M.).

- [1] Voit J 1995 *Rep. Prog. Phys.* **58** 977
- [2] Giamarchi T 2003 *Quantum Physics in One Dimension* (New York: Oxford University Press)
- [3] Schönhammer K 2005 in *Interacting Electrons in Low Dimensions* ed. by D. Baeriswyl (Dordrecht: Kluwer Academic Publishers)
- [4] For a review on the experimental status until 2009 see: Grioni M, Pons S and Frantzeskakis E 2009 *J. Phys.: Condens. Matter* **21** 023201
- [5] Theumann A 1967 *J. Math. Phys.* **8** 2460
- [6] Dzyaloshinskii IE and Larkin AI 1973 *Zh. Eksp. Teor. Fiz.* **65** 411 (english translation: 1974 *Sov. Phys.-JETP* **38** 202)
- [7] Luther A and Peschel I 1974 *Phys. Rev. B* **9** 2911
- [8] Meden V and Schönhammer K 1992 *Phys. Rev. B* **46** 15753
- [9] Schönhammer K and Meden V 1993 *Phys. Rev. B* **47** 16205
- [10] Voit J 1993 *Phys. Rev. B* **47** 6740
- [11] Schönhammer K and Meden V 1993 *J. Electr. Spectrosc. Relat. Phenom.* **62** 225
- [12] Haldane FDM 1981 *J. Phys. C* **14** 2585
- [13] Sóllyom J 1979 *Adv. Phys.* **28** 209
- [14] Kane CL and Fisher MPA 1992 *Phys. Rev. B* **46** 15233
- [15] Fabrizio M and Gogolin AO 1995 *Phys. Rev. B* **51** 17827
- [16] Eggert S, Johannesson H and Mattsson A 1996 *Phys. Rev. Lett.* **76** 1505
- [17] Grap S and Meden V 2009 *Phys. Rev. B* **80** 193106
- [18] Ishii H, Kataura H, Shiozawa H, Yoshioka H, Otsubo H, Takayama Y, Miyahara T, Suzuki S, Achiba Y, Nakatake M, Narimura T, Higashiguchi M, Shimada K, Namatame H and Taniguchi M 2003 *Nature* **426** 540
- [19] Hager J, Matzdorf R, He J, Jin R, Mandrus D, Cazalilla MA and Plummer EW 2005 *Phys. Rev. Lett.* **95** 186402
- [20] Wang F, Alvarez JV, Mo S-K, Allen JW, Gweon G-H, He J, Jin R, Mandrus D and Höchst H 2006 *Phys. Rev. Lett.* **96** 196403
- [21] Jompol Y, Ford CJB, Griffiths JP, Farrer I, Jones GAC, Anderson D, Ritchie DA, Silk TW and

- Schofield AJ 2009 *Science* **325** 597
- [22] Blumenstein C, Schäfer J, Mietke S, Meyer S, Dollinger A, Lochner M, Cui XY, Pattthey L, Matzdorf R and Claessen R 2011 *Nature Physics* **7** 776
- [23] Meden V 1999 *Phys. Rev. B* **60** 4571
- [24] Imambekov A, Schmidt TL and Glazman LI 2011 arXiv:1110.1374
- [25] Metzner W, Salmhofer M, Honerkamp C, Meden V and Schönhammer K 2011 arXiv:1105.5289, to be published in *Rev. Mod. Phys.*
- [26] Schuricht D, Essler FHL, Jaefari A and Fradkin E 2008 *Phys. Rev. Lett.* **101** 086403; 2011 *Phys. Rev. B* **83** 035111; Schuricht D 2011 *Phys. Rev. B* **84** 045122
- [27] Bockrath M, Cobden DH, Lu J, Rinzler AG, Smalley RE, Balents L and McEuen PL 1999 *Nature* **397** 598
- [28] Rodin AS and Fogler MM 2010 *Phys. Rev. Lett.* **105** 106801
- [29] Eggert S 2000 *Phys. Rev. Lett.* **84** 4413
- [30] Preus R, Muramatsu A, von der Linden W, Dieterich P, Assaad FF and Hanke W 1994 *Phys. Rev. Lett.* **73** 732
- [31] Benthien H 2005 PhD thesis, Universität Marburg
- [32] Benthien H, Gebhard F and Jeckelmann E 2004 *Phys. Rev. Lett.* **69** 256401
- [33] Abendschein A and Assaad FF 2006 *Phys. Rev. B* **73** 165119
- [34] Jeckelmann E 2011 arXiv:1111.6545 and this special issue
- [35] Enss T, Meden V, Andergassen S, Barnabé-Thériault X, Metzner W and Schönhammer K 2005 *Phys. Rev. B* **71** 155401
- [36] Andergassen S, Enss T, Meden V, Metzner W, Schollwöck U and Schönhammer K 2006 *Phys. Rev. B* **73** 045125
- [37] Essler FHL, Frahm H, Göhmann F, Klümper A and Korepin VE 2005 *The One-Dimensional Hubbard Model* (Cambridge: Cambridge University Press)
- [38] Schulz HJ 1990 *Phys. Rev. Lett.* **64** 2831
- [39] Ejima S, Gebhard F and Nishimoto S 2005 *Europhys. Lett.* **70** 492
- [40] Meden V, Metzner W, Schollwöck U, Schneider O, Stauber T, and Schönhammer K 2000 *Eur. Phys. J. B* **16** 631
- [41] Andergassen S, Enss T, Meden V, Metzner W, Schollwöck U, and Schönhammer K 2004 *Phys. Rev. B* **70** 075102
- [42] Governale M and Zülicke U 2004 *Solid State Com.* **131** 581
- [43] Schulz A, De Martino A, Ingenhoven P and Egger R 2009 *Phys. Rev. B* **79** 205432
- [44] Schulz A, De Martino A and Egger R 2010 *Phys. Rev. B* **82** 033407
- [45] Meyer S, Schäfer J, Blumenstein C, Höpfner P, Bostwick A, McChesney JL, Rotenberg E, Claessen R 2011 *Phys. Rev. B* **83** 121411(R)
- [46] Egger R and Gogolin AO 1997 *Phys. Rev. Lett.* **79** 5082
- [47] Kane C, Balents L and Fisher MPA 1997 *Phys. Rev. Lett.* **79** 5086